A Compact Wideband Microstrip Crossover

Wendong Liu, Zhijun Zhang, *Senior Member, IEEE*, Zhenghe Feng, *Senior Member, IEEE*, and
Magdy F. Iskander, *Fellow, IEEE*

***Abstract*—In this letter, a planar microstrip crossover junction is presented. The conductor-backed coplanar waveguide (CB-CPW) structure with vias is employed as the core part of the crossover design. The dimensions of the CB-CPW crossover itself are 11.3 × 11.3 mm^2. Two kinds of the transitions between the microstrip line (MSL) and the CB-CPW structure are merged into a double side print circuit board. This presented crossover junction has a bandwidth from 10 up to 6000 MHz for 20 dB return loss, 1 dB insertion loss and −20 dB isolation. Compared with the other designs, this planar crossover features wide bandwidth and compact configuration.**

***Index Terms*—Coplanar waveguide (CPW) with ground, microstrip crossover, transmission line, microstrip to conductor-backed (CB)-CPW transition.**

I. INTRODUCTION

WITH the rapid development of microwave and millimeter-wave integrated circuits, crossover is frequently employed while designing multi-channel systems or antenna array feeds such as butler matrix. Theoretical analyses of air-bridge crossover structures are presented in [1] and [2]. In practice, a finite ground coplanar (FGC) waveguide crossover with a wide operating band from dc to 40 GHz is proposed in [3]. However, the Air Bridge needs special treatments, such as bonding wire or MEMS processing, which are not compatible with the normal planar circuit techniques. The basic solution in [4] is to cascade two branch-line directional couplers. However, the size of the coupler, based on a $\lambda/4$ square, will be difficult to satisfy in a low frequency band. Hence, a modified version which is based on the same principle is proposed in [5]. This particular design works at 1 GHz, with a 250 MHz bandwidth and a size of 35×35 mm^2. Other similar planar structures have also been proposed and studied including disk circuits [6], double-ring [7] and cross-ring [8]. To meet the need of dual-band and multiband operation, a microstrip crossover operating at 790 and 1195 MHz is presented in [9] with a 35 MHz bandwidth (both upper and lower band) and a size of 62.2×53.3 mm^2. In [10], a crossover operating across the band of 3 to 10 GHz is realized by cascading two conductor backed coplanar waveguide slot couplers, whereas it is a multilayer structure.

From the above, it may be noted that most of the crossovers in fully planar structures are of narrow bandwidth because the designs are based on couplers. Others obtain wideband at the expense of multi-layer and complicated structure. Bandwidth is a disadvantage for most planar crossovers. To tackle this problem, a compact and wideband microstrip crossover is presented in this letter. The crossover merges two orthogonally placed CB-CPWs and two kinds of transitions between microstrip and CB-CPW into a double side print circuit board (PCB). The dimensions of the CB-CPW crossover itself are 11.3×11.3 mm^2. For verification, both simulated and measured performances of the proposed crossover junction are shown in this letter.

II. MICROSTRIP CROSSOVER JUNCTION DESIGN

The 3-D layout of the proposed microstrip crossover junction is shown in Fig. 1. The circuit is realized on a low cost Teflon substrate with a dielectric constant of 2.65 and dimensions of $30 \times 30 \times 0.8$ mm^3. All the four ports are designed to be 50 Ω. For the substrate adopted in the design, the width of a 50 Ω MSL is 2.15 mm. As shown in Fig. 1, for Port 1 and Port 3, a short transition line is employed to connect the 50 Ω MSL and the CB-CPW structure. For Port 2 and Port 4, via holes with a radius of 0.5 mm connect the MSL to the central conductor of the CB-CPW on Layer 2 to realize the transition. The position of the two via holes is 8 mm away from the edge and the gap W_1 is set to be 0.75 mm for a better transition performance. It should be noticed that both the transitions introduce discontinuities. Hence, to achieve better matching results, the characteristic impedance of CB-CPW is set to be about 55 Ω, not 50 Ω. The width of the central conductor W is set to 1.5 mm and the slot gap S of the CB-CPW is 0.25 mm.

The two CB-CPWs are placed orthogonally to each other, guaranteeing the isolation between the adjacent ports. The ground planes are reused, which means that the bottom ground plane of one CB-CPW serves as the side ground plane of the other CB-CPW, and vice versa. Fig. 2 shows the E-field distributions at different cross sections defined in Fig. 1. As shown in Fig. 2, when propagating into the core part, the MSL mode needs to be converted to the CB-CPW mode. Due to the existence of the bottom ground, the CB-CPW mode gets more similar to the MSL mode, which makes the transition easier and minimizes the reflection. Vias with radius of 0.4 mm short the side ground to the bottom ground and the main function is to guarantee that the CB-CPW mode can be excited by the MSL,

Manuscript received November 25, 2011; revised February 20, 2012; accepted February 28, 2012. Date of publication April 17, 2012; date of current version May 04, 2012. This work was supported by the National Basic Research Program of China under Contract 2010CB327400, in part by the National High Technology Research and Development Program of China (863 Program) under Contract 2011AA010202, the National Natural Science Foundation of China under Contract 60771009, the National Science and Technology Major Project of the Ministry of Science and Technology of China 2010ZX03007-001-01 and Tsinghua-QUALCOMM associated Research Plan.

W. Liu, Z. Zhang and Z. Feng are with the State Key Lab of Microwave and Communications, Tsinghua National Laboratory for Information Science and Technology, Tsinghua University, Beijing, 100084, China (e-mail: zjzh@tsinghua.edu.cn).

M. F. Iskander is with HCAC, University of Hawaii at Manoa, Honolulu, HI 96822 USA (e-mail: iskander@spectra.eng.hawaii.edu).

Digital Object Identifier 10.1109/LMWC.2012.2190270

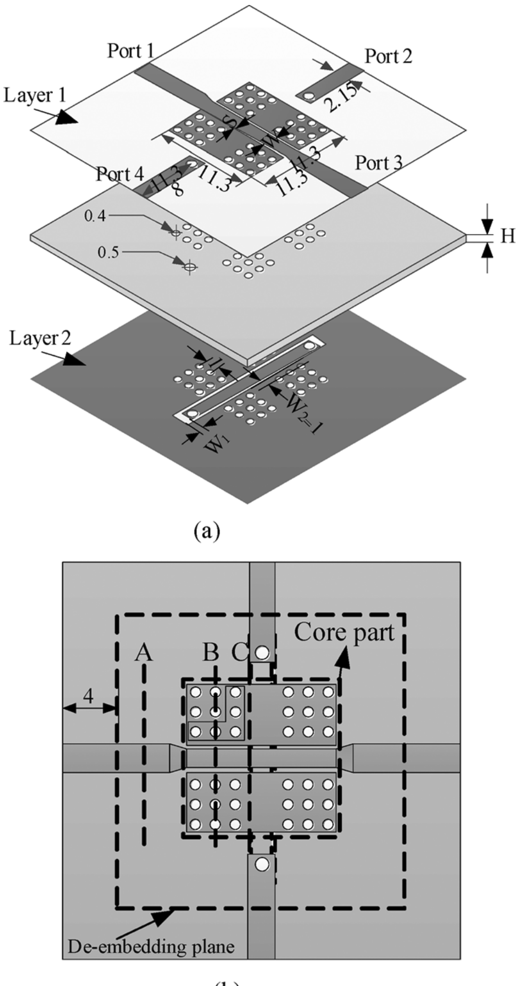

Fig. 1. (a) 3-D Layout of the proposed microstrip crossover junction. (b) Front view (Unit: mm).

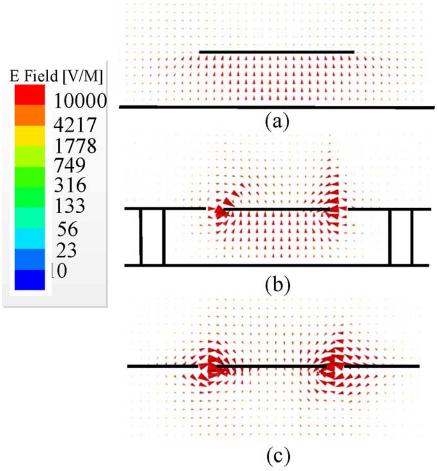

Fig. 2. E field distributions at cross section(a) A. (b) B. (c) C.

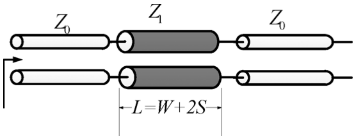

Fig. 3. Model of the discontinuity in CB-CPW crossover.

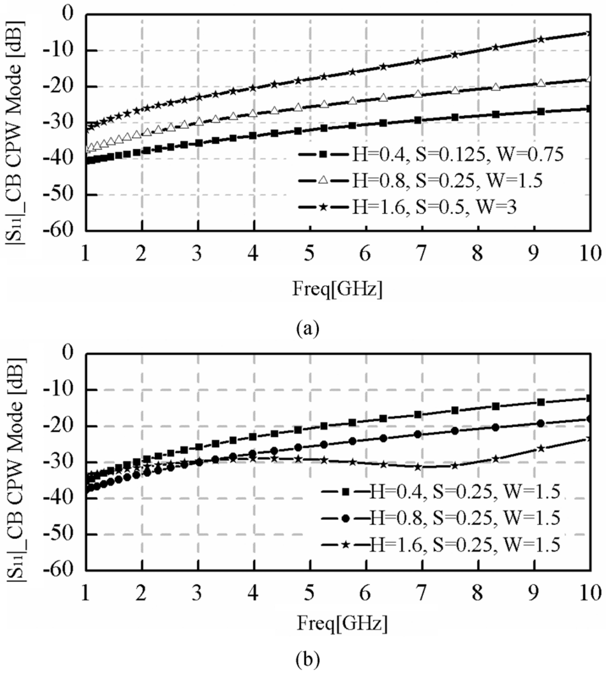

Fig. 4. Simulated reflection coefficients of the CB-CPW crossover without transition to MSL (the core part). (a) variation in S, W and H with the same ratio. (b) variation only in H (Unit: mm).

especially for the first row of the vias closest to the slots of the CB-CPW. Other vias have little effect on the performance of the crossover. The parameter W_2 (the position of the first row of the vias) also affects the characteristic impedance of the CB-CPW. The distance between the vias is adjusted to make sure that the vias serve as a shorting wall. At the cross section C, the slots cut off the current on the bottom ground of the CB-CPW. Because most of the CB-CPW mode's energy is confined in the two slots of the CB-CPW, the reflection caused by the discontinuity on the bottom ground is minimized. This effect can be analyzed approximately by inserting a short transmission line in CPW mode with characteristic impedance Z_1 into the CB-CPW with characteristic impedance Z_0 as shown Fig. 3. In theory, the matching gets worse as L gets larger. Fig. 4 shows simulated reflection coefficients for the CB-CPW crossover itself without transition to the MSL. To change L while maintaining Z_0 and Z_1, W, S and H need to be changed simultaneously with the same ratio. As indicated in Fig. 4(a), wider bandwidth is achieved as L gets smaller. Fig. 4(b) shows the simulated reflection coefficients at Port 1 when only H changes. As H gets smaller, the current on the bottom ground gets stronger and thus the reflection caused by the discontinuity on the bottom ground gets stronger. Fig. 5 shows the simulated reflection coefficients at Port 2 with the variation in S only. It should be noticed that smaller slot gap does not mean wider bandwidth. Impedance matching between the MSL and CB-CPW should also be considered.

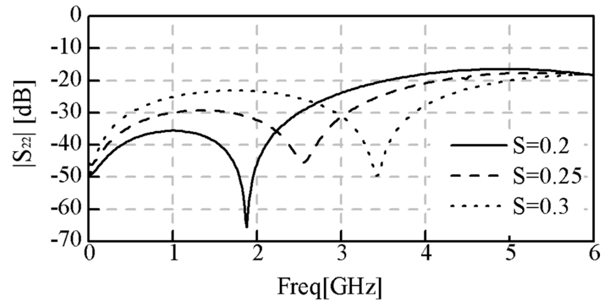

Fig. 5. Simulated reflection coefficients at Port 2 of the whole structure with the variation in S $(H = 0.8, W = 1.5)$.

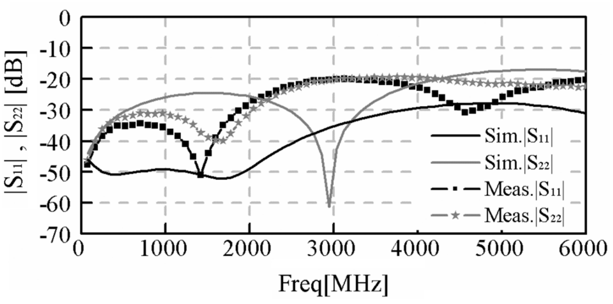

Fig. 6. Simulated and measured reflection coefficients of the crossover.

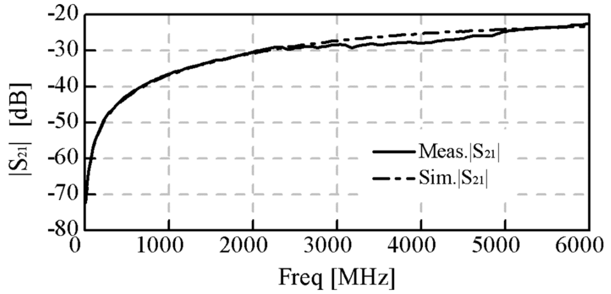

Fig. 7. Simulated and measured isolation results of the crossover.

III. RESULTS

Due to limitation of the measurement equipment, the prototype is tested only from 10 MHz to 6000 MHz. All the measured results are de-embedded to the plane shown in Fig. 1(b) to eliminate the influence of the connectors. Fig. 6 shows the simulated and measured magnitudes of S_{11} and S_{22}. Similar results are also obtained at Port 3 and 4. The differences between the simulated and measured results are mainly caused by the accuracy of the fabrication. The measured magnitude of reflection coefficient smaller than -20 dB is from 10 to 6000 MHz for the four ports. Referring to Fig. 7, the isolation between the adjacent ports is better than -20 dB across the entire measured band from 10 to 6000 MHz. As indicated in Fig. 7, the electric length of the gap S gets larger as the frequency goes up and results in the degradation of the isolation. The simulated and measured insertion losses are lower than 1 dB across the entire measured band and agree well as shown in Fig. 8.

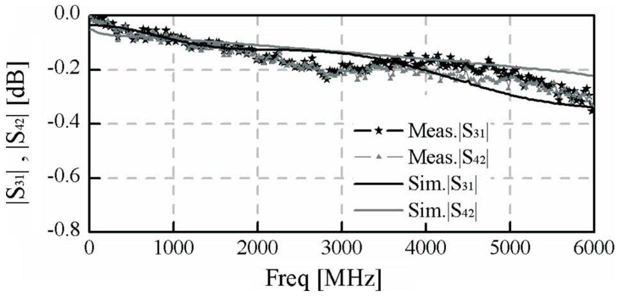

Fig. 8. Simulated and measured insertion loss of the crossover.

IV. CONCLUSION

In this letter, a compact microstrip crossover junction is designed, fabricated and measured. To achieve the crossover function in a planar structure, the junction merges two orthogonally placed CPWs and two kinds of transitions between MSL and CB-CPW into a double side PCB. According to the simulated and measured results, this crossover junction features both wide working bandwidth (from 10 to 6000 MHz) and compact structure and could be used in designing multi-channel systems or antenna arrays.

REFERENCES

[1] S. C. Wu, H. Y. Yang, N. G. Alexopoulos, and I. Wolff, "A rigorous dispersive characterization of microstrip cross and T junctions," *IEEE Trans. Microw. Theory Tech.*, vol. 38, no. 12, pp. 1837–1844, Dec. 1990.

[2] T.-S. Horng, "A rigorous study of microstrip crossovers and their possible improvement," *IEEE Trans. Microw. Theory Tech.*, vol. 42, no. 9, pp. 1802–1806, Sep. 1994.

[3] G. E. Ponchak and E. Tentzeris, "Development of finite ground coplanar (FGC) waveguide 90 degree crossover junctions with low coupling," *IEEE MTT-S Int. Dig.*, vol. 3, pp. 1891–1894, 2000.

[4] M. M. Alam, "Microstrip antenna array with four port butler matrix for switched beam base station application," in *Proc. Int. Conf. Comp. Inform. Technol.*, 2009, pp. 531–536.

[5] X. Liu, C. P. Yu, Y. A. Liu, S. L. Li, F. Wu, and M. Su, "A novel compact planar crossover with simple design procedure," in *Proc. Asia-Pacific Microw. Conf.*, 2010, pp. 1633–1636.

[6] K. C. Gupta and M. D. Abouzahra, "Analysis and design of four-port and five-port microstrip disk circuits," *IEEE Trans. Microw. Theory Tech.*, vol. MTT-33, no. 12, pp. 1422–1428, Dec. 1985.

[7] Y. Chen and S. P. Yeo, "A symmetrical four-port microstrip coupler for crossover application," *IEEE Trans. Microw. Theory Tech.*, vol. 55, no. 11, pp. 2434–2438, Nov. 2007.

[8] Y. C. Chiou, J. T. Kuo, and H. R. Lee, "Design of compact symmetric four-port crossover junction," *IEEE Microw. Wireless Compon. Lett.*, vol. 19, no. 9, pp. 545–547, Sep. 2009.

[9] F.-L. Wong and K.-K. M. Cheng, "A novel, planar, and compact crossover design for dual-band applications," *IEEE Trans. Microw. Theory Tech.*, vol. 59, no. 3, pp. 568–573, Mar. 2011.

[10] M. Nedil, A. M. Habib, and T. A. Denidni, "Novel ultra-wideband CB-CBW butler matrix," in *Proc. IEEE Antennas Propag. Soc. Int. Symp.*, 2008, pp. 1–4.